Compact Single-Port Harmonic Transponder for Backscattering Communications and Energy Harvesting Applications

Jinyao Zhang, Sumin David Joseph, Yi Huang, *Fellow, IEEE*, and Jiafeng Zhou

***Abstract*— This article proposes a novel architecture for the design of a single-port harmonic transponder. The need for a diplexer is eliminated by adding a quarter-wave and a one-eighth-wave transmission line, combined with the two quarter-wave stubs that are usually needed in a conventional harmonic transponder. The proposed architecture provides isolation between the fundamental and the second harmonic signals and sends them to the desired port, while only introducing extremely low insertion loss. Compared with a single-resonator-based diplexer, it has a much wider bandwidth and a much more compact size than the conventional dual-port design. The proposed diplexing structure can also be used in the design of a compact single-port harmonic transponder with dc power supply capability. With such a design, the harmonic transponder can not only generate harmonics for communication purposes, but also provide power for the operation of communication modules, while being small in size and working with a single antenna. A harmonic tag with a simple modulation module based on this architecture is designed to demonstrate its practical value. The proposed design can work at a low input power level and is very suitable for future low-power Internet of Things (IoT) applications.**

***Index Terms*— Harmonic transponder, Internet of Things (IoT), radio frequency identification (RFID), RF energy harvesting, Schottky diode.**

I. Introduction

With the popularization of the Internet of things (IoT) and wireless sensor networks in life, Radio Frequency Identification (RFID) as a successful technology plays an increasingly important role in tagging, tracking, sensing, and locating objects [1]. Conventional RFID systems utilize a single frequency for interrogation and return, which can cause unwanted self-jamming or clutter noise interference from environmental reflection. Harmonic backscattering-based RFID tags operate in two frequency bands, one for the uplink and the other, usually the second harmonic, for the downlink.

Manuscript received 11 October 2022; revised 6 December 2022 and 6 January 2023; accepted 11 January 2023. This work was supported in part by the Royal Society under Grant IEC\NSFC\181364. *(Corresponding author: Jiafeng Zhou.)*

Jinyao Zhang, Yi Huang, and Jiafeng Zhou are with the Department of Electrical Engineering and Electronics, University of Liverpool, L69 3GJ Liverpool, U.K. (e-mail: jinyao.zhang@liverpool.ac.uk; yi.huang@liverpool.ac.uk; jiafeng.zhou@liverpool.ac.uk).

Sumin David Joseph is with the Department of Electronic and Electrical Engineering, University of Sheffield, S10 2TN Sheffield, U.K. (e-mail: s.d.joseph@sheffield.ac.uk).

Color versions of one or more figures in this article are available at https://doi.org/10.1109/TMTT.2023.3239259.

Digital Object Identifier 10.1109/TMTT.2023.3239259

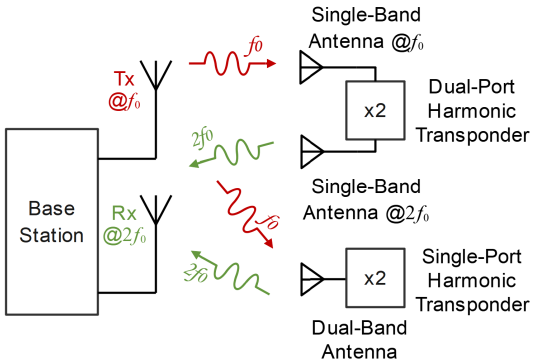

Fig. 1. Block diagram of a harmonic transponder system with a dual-port and a single-port topology.

Thus, clutter noise interference at the fundamental frequency can easily be filtered out at the interrogator side. This advantage makes harmonic backscattering a potential solution for long-range RFID tags in cluttered environments. Due to their small size, low cost, anti-jamming, and battery-less features, harmonic RFID tags have been used in scenarios such as collision avoidance systems [2], miniature trackers [3], and disaster victim detection [4], [5] to avoid strong harmful reflection. Recently, passive wireless sensors based on harmonic RFID tags have been reported for backscattering communications at extremely low power levels [6], [7].

The frequency conversion of a passive harmonic transponder can be realized by a nonlinear component (usually a diode). As Fig. 1 shows, the conventional transponder is usually a dual-port one with a pair of antennas for receiving and transmitting, respectively. The fundamental frequency signal transmitted from the base station is received by the receiving antenna at the harmonic transponder which is then converted into harmonics and sent back by another antenna.

Conversion loss will reduce the output harmonic power, thus affecting the usable distance of harmonic RFID tags. In other words, the conversion efficiency largely determines the performance of harmonic transponders. It requires good cooperation between the frequency conversion part and the antenna part. To achieve good performance, high isolation between the transmitting and receiving antennas is needed, limiting the flexibility of antenna design.

Several publications reported attempts at single-port transponder designs to alleviate the limitations of transponders with two independent antennas. In [8], a diplexer-based

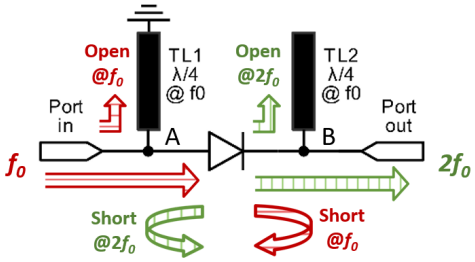

Fig. 2. Energy flow of the conventional dual-port harmonic transponder.

single-port transponder architecture is proposed, that allowed it to operate simply with a single dual-band antenna, helping to reduce the number of antennas. The design could combine the input and output ports of the conventional dual-port harmonic transponder while providing significant isolation. Since the diplexer was based on a single resonator design, the limited bandwidth made it highly sensitive to manufacturing errors. In [9], a single-port design based on a third-order hairpin diplexer is proposed to enhance the bandwidth, but it also entailed additional circuit area.

In this work, a new architecture of a single-port harmonic transponder with a stub-based diplexing structure is proposed and analyzed. A one-eighth-wave and a quarter-wave transmission line are added in addition to the two quarter-wave stubs in the conventional harmonic transponder. They allow the fundamental frequency f_0 and the second harmonic $2f_0$ to flow in the desired directions while providing significant isolation between them. Thus, it is possible to convert two ports to a single one with only a minimal increase in circuit area. The proposed diplexing structure has a wider bandwidth with low sensitivity to fabrication errors than using a single-resonator-based diplexer. The design is also suitable for applications combining wireless power transfer with harmonic backscatter communications, capable of simultaneously harvesting wireless RF energy and generating harmonics.

The rest of the article is organized as follows. Section II explains the working principle of the proposed single-port harmonic transponder. One example of the proposed single-port harmonic transponder is presented in Section III with simulation and measurement results. Section IV includes two parts: the first part describes the design of a single-port harmonic transponder with dc power supply capability; the second part demonstrates a backscattering system that makes use of harvested energy to modulate the second harmonic for communication purposes. Finally, a conclusion is drawn in Section V.

II. Topology and Theoretical Analysis

Fig. 2 shows a schematic of the conventional dual-port passive harmonic transponder and the energy flow of the fundamental and the second harmonic. The red arrow with horizontal stripes denotes the energy flow path of the fundamental wave, and the green one with vertical stripes denoted the second harmonic. The inherent nonlinearity of the diode will produce higher-order harmonics. To enhance the second harmonic conversion efficiency of the diode, a short-circuited and an open-circuit quarter-wave stub (named TL_1 and TL_2)

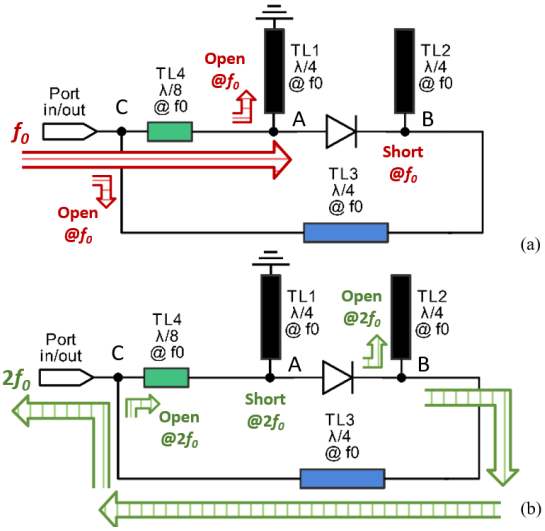

Fig. 3. Energy flow of the proposed single-port harmonic transponder at: (a) fundamental frequency f_0 and (b) second harmonic $2f_0$.

at the fundamental frequency f_0 are placed on the two sides of the diode, respectively. The quarter-wave short-circuited stub TL_1 at the input side presents an open circuit at the fundamental frequency. It allows the injected fundamental signal to reach the diode. But it acts as a short-circuited at the second harmonic. That is, the second harmonic is shorted at Point A. At Point B, the quarter-wave open-circuit stub TL_2 short-circuits the fundamental frequency without affecting the second harmonic. This is because the open-circuit quarter-wave stub at f_0 is the half wavelength at $2f_0$. So the second harmonic TL_2 is still an open circuit, but the fundamental frequency will be reflected by the short-circuited at Point B.

To enable the transponder's input and output to share one port without using a diplexer, a one-eighth-wave transmission line TL_4 (at f_0) is added between Point C and TL_1. The transponder's output is connected to Point C by a quarter-wave transmission line TL_3 (at f_0). Fig. 3(a) and (b) show the paths of signals at the fundamental frequency and the second harmonic frequency in the proposed dual-port passive harmonic transponder, respectively. Like the conventional dual-port design, the stub TL_1 at the input side makes Point A an open circuit at the fundamental frequency and short-circuited at the second harmonic. The added transmission line TL_4 between Points C and A is one-eighth wave long at f_0 and quarter-wave long at $2f_0$. This added quarter-wave transmission line will transform the short-circuited at the second harmonic into an open circuit, but it does not affect transmission at the fundamental frequency. That is, at the second harmonic frequency, TL_4 makes the input impedance infinity, seeing from Point C toward the diode. It will only cause some phase changes with very little insertion loss to the fundamental frequency signal. Hence, the added transmission line has very little effect on the operation of the diode.

The quarter-wave open-circuit stub TL_2 at the output side makes Point B short-circuited at the fundamental frequency and open circuit at the second harmonic frequency. Thanks to TL_3 ($\lambda/4$ long at f_0) between Points C and B, at the fundamental frequency, the input impedance seen from Point C to B

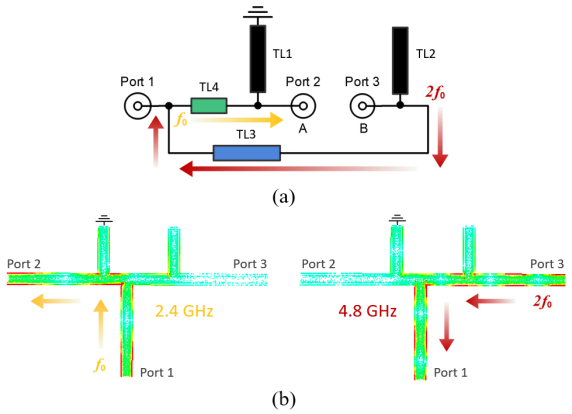

Fig. 4. (a) Schematic of a simplified model of the proposed diplexing structure. (b) Current distribution of the proposed diplexing structure at the fundamental and second-harmonic frequencies.

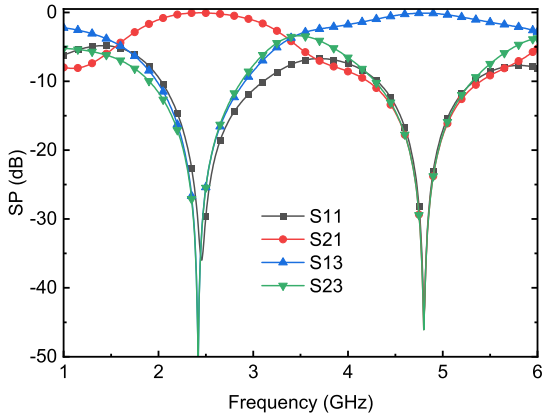

Fig. 5. Simulated S-parameters of the simplified model of the proposed diplexing structure.

through TL_3 will be infinite. And this TL_3 is half-wavelength long at the second harmonic, so it has no effect on the transmission of the second harmonic from the output side of the diode to the port. To put it another way, the second harmonic signal can be transmitted with ultralow loss from the diode output to the output of the harmonic transponder via the half-wave transmission line. But no power from the input port at the fundamental frequency will go through this transmission line to the output side of the diode.

To better demonstrate the performance of the proposed diplexing structure, the diode in Fig. 3 is removed and Points A and B are virtualized into two ports, as shown in Fig. 4(a). Point A at the input of the diode is designated as Port 2, and Point B at the other end is Port 3. And Port 1 is the main input and output port as Point C in Fig. 3, which is used to connect the antenna to receive the fundamental frequency signal and transmit the second harmonic signal. The yellow and red arrows indicate the direction of transmission of the fundamental frequency and second harmonic, respectively. The current distributions at f_0 and $2f_0$ of the proposed diplexing structure are shown in Fig. 4(b). The signal at the fundamental frequency injected from the Port 1 reaches Port 2 only through the one-eighth-wave transmission line TL_4, and does not reach Prot 3 through TL_3, as indicated by the yellow arrow in Fig. 4(b). On the contrary, the second harmonic from Port 3 will pass through the added quarter-wave transmission line

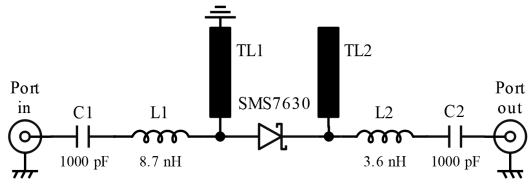

Fig. 6. Schematic of the designed conventional dual-port harmonic transponder.

TL_3 and reaches Port 1 without being injected into Port 2. Therefore, the proposed diplexing structure can easily control the transmission direction of the fundamental frequency and the second harmonic and provide isolation between them. That is, the passive harmonic transponder based on this structure enables the input and output to share a port for communication without mutual influence.

This simplified model of the proposed diplexing structure was simulated using the Advanced Design System (ADS) and the S-parameter results are shown in Fig. 5. The yellow line (S_{21}) and the red line (S_{13}) show the transmission coefficient from Port 1 to 2 and from Port 3 to 1, respectively. The results show that the insertion loss from Port 1 to 2 at 2.4 GHz and from Port 3 to 1 at 4.8 GHz are both less than 0.6 dB. The proposed diplexing structure achieved fractional bandwidths of more than 50% at 2.4 GHz and 30% at 4.8 GHz in simulation, which has a wider passband than the single-resonator-based diplexer [7]. The isolation between Ports 2 and 3 as the green line shows (S_{23}) is over 30 dB at both frequencies. Since the design is based on quarter-wave and one-eighth-wave transmission lines, the length of the transmission lines can be quickly estimated based on the desired operating frequency, and their exact sizes are obtained by subsequent co-optimization with other parts of the circuit.

III. Compact Single-Port Harmonic Transponder

A. Circuit Design

A conventional dual-port harmonic transponder working at the fundamental frequency of 2.4 GHz was designed first. As shown by the circuit diagram in Fig. 6, the conventional architecture consists of a Schottky diode, two quarter-wave stubs, and input and output matching networks [10]. C_1 and C_2 as dc blocking capacitors are placed at the input and output ports. A Schottky barrier diode SMS7630 with a low threshold voltage from Skyworks is chosen. Both matching networks are based on a single inductor to compensate for the junction capacitance and package capacitance of the diode to tune the impedances of input and output at the operating frequency. Using a single inductor instead of a complicated matching circuit can minimize the size of the circuit board [11]. A quarter-wave short-circuited stub TL_1 and a quarter-wave open-circuit stub TL_2 are placed on both sides of the diode.

Based on the analysis in Section II, by adding a quarter-wave transmission line TL_3 (at f_0) and a one-eighth-wave transmission line TL_4 (at f_0) to the conventional harmonic transponder, the two ports can be combined into a single one. The proposed transponder is shown in Fig. 7. The lengths of TL_3 and TL_4 have been co-optimized with the complete circuit to compensate for the phase effect from lumped elements in the circuit.

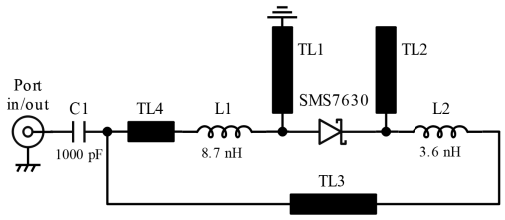

Fig. 7. Schematic of the proposed single-port harmonic transponder.

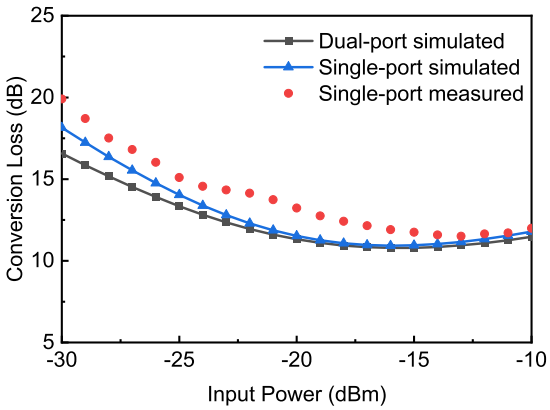

Fig. 8. Comparison of simulated and measured conversion loss of the designed conventional dual-port and the proposed single-port harmonic transponder.

The performance of the conventional dual-port harmonic transponder and the proposed single-port one were simulated using ADS. Fig. 8 shows the harmonic transponder power conversion loss CL, which is calculated by

$$\mathrm{CL(in\ dB)} = P_{f_0}(\mathrm{dBm}) - P_{2f_0}(\mathrm{dBm}) \tag{1}$$

where P_{f0} is the incident power at the fundamental frequency in dBm and P_{2f0} is the output power of the transponder at the second harmonic frequency. The black line shows the simulated result of power conversion loss of the transponder with two ports. The blue line shows the conversion loss with a single port. When the input power range is between -25 and -10 dBm, there is no significant difference between them. It can be shown that the proposed diplexing structure has little effect on the diode operation and does not increase the conversion loss. Fig. 9 shows the conversion loss of the conventional dual-port and the proposed single-port harmonic transponder in the frequency range of 2.2–2.6 GHz. When the dual ports are converted to a single port, the bandwidth is slightly narrower, but it has a very low impact on conversion loss near the center frequency.

B. Measurement and Comparison

For evaluating the performance of the proposed single-port harmonic transponder, a prototype is fabricated on a Rogers RO4003C substrate with a relative permittivity ε_r of 3.55 and a thickness of 1.524 mm. A photograph of the fabricated prototype is shown in Fig. 10. The transmission lines are meandered where possible to save space. The size of the circuit board is only 12 mm long and 10 mm wide.

Here, three antennas were used to carry out the far-field measurement to characterize the overall performance of the

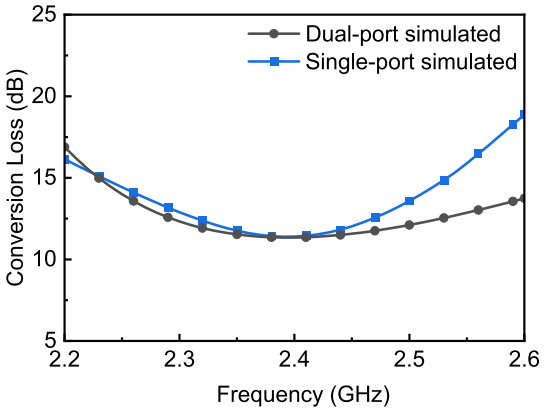

Fig. 9. Simulated conversion loss versus frequency of the designed conventional dual-port and the proposed single-port harmonic transponder with an input power of -15 dBm.

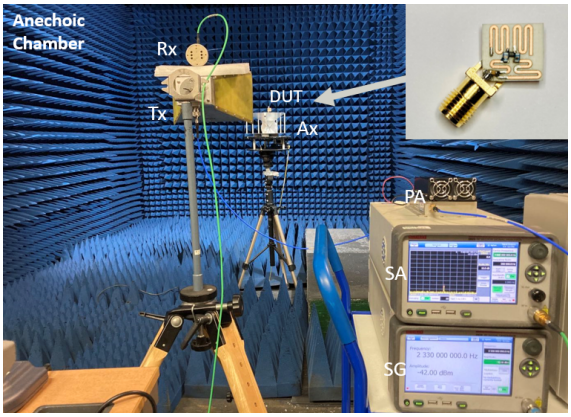

Fig. 10. Photographs of the measurement setup and the fabricated prototype of the proposed single-port harmonic transponder.

proposed single-port harmonic transponder. The photograph of the measurement setup in an anechoic chamber is shown in Fig. 10. To measure the conversion loss of the proposed transponder accurately, three standard gain waveguide horn antennas were used. On the base station side, the Tx antenna was an HF906 antenna from Rohde and Schwarz and the Rx was an SH2000 antenna from MVG [13]. On the transponder side, the antenna Ax used for both receiving and transmitting was an SH1000 antenna also from MVG. In the measurement, the distance between the Tx/Rx antennas and the Ax antenna was set to be 1.8 m, which satisfied the far-field condition at 2.4 GHz. A Keithley 2920 RF signal generator was used to generate 2.4 GHz signals with a maximum output power of 13 dBm. A 20 W power amplifier was used to amplify the signal to ensure that the signal level received by the transponder covered all the input power levels that needed to be measured. A low pass filter was added between the power amplifier and the Tx antenna to reduce the influence of the harmonic power generated by the amplifier on the measurement results. The Rx antenna was connected to a signal analyzer to display the received second harmonic from the transponder. The calculation of the link budget is based on the Friis transmission formula [12]. The conversion loss (in dB) at the proposed transponder is calculated by

$$\mathrm{CL} = P_r - P_t - G_{f_0}^{\mathrm{Tx}} - G_{2f_0}^{\mathrm{Rx}} - G_{f_0}^{\mathrm{Ax}} - G_{2f_0}^{\mathrm{Ax}} - \mathrm{PL}_{f_0} - \mathrm{PL}_{2f_0} \tag{2}$$

TABLE I
COMPARISON OF THE PROPOSED HARMONIC TRANSPONDER AND RELATED DESIGNS

Reference	2017 [7]	2019 [8]	2021 [9]	**This work**
Frequency GHz	1.2	3.5	3.5	**2.4**
Diode	HSMS-2850	SMS-7630	SMS-7621	**SMS-7630**
Port	Dual port	Single port	Single port	**Single port**
Type of Ports Combination	-	single-resonator-based diplexer	Third-order hairpin diplexer	**Diplexing structure**
Size λ_0	0.032 × 0.112	0.280 × 0.280	0.542 × 0.635	**0.080 × 0.096**
Conversion loss @-25 dBm	26.5 dB	17 dB	14 dB	**15 dB**

where P_r is the power received by the Rx antenna, P_t is the power transmitted by the Tx antenna, $G_{f_0}^{\mathrm{Tx}}$ is the gain of the Tx antenna at f_0, $G_{2f_0}^{\mathrm{Rx}}$ is the gain of the Rx antenna at $2f_0$, $G_{f_0}^{\mathrm{Ax}}$ and $G_{2f_0}^{\mathrm{Ax}}$ are the gain of the Ax antenna at f_0 and $2f_0$, and PL_{f_0} and PL_{2f_0} are the free-space path loss (FSPL) at f_0 and $2f_0$, respectively. The FSPL in dB is defined as

$$\mathrm{FSPL} = 20\log_{10}\left(\frac{4\pi df}{c}\right) \tag{3}$$

where d is the distance between the Tx and Rx antennas, f is the frequency of the signal, and c is the speed of light.

The red dotted line in Fig. 8 shows the measured conversion loss of the proposed harmonic transponder. The insertion loss of the cables and connectors has been taken into account in the measurement. It can be observed that the measured results agree well with the simulated ones. When the input power is between −30 and −10 dBm, the transponder can achieve a conversion loss of no more than 20 dB. The proposed harmonic transponder has a stable conversion loss in a dynamic input power range of at least 15 dB (from −25 to −10 dBm).

Table I compares the performance of the proposed single-port harmonic transponder with previous works. The proposed design is the smallest among single-port transponders. A lower conversion loss is achieved at an input power of −25 dBm, which proves that the proposed diplexing structure does not add additional power loss.

IV. COMPACT SINGLE-PORT HARMONIC TRANSPONDER WITH DC POWER SUPPLY CAPABILITY

A typical passive harmonic transponder can generate harmonics for communication purposes. Some attempts to append information to harmonics by modulation have been reported in the literature [14], [15]. But for applications that require specific identifier information or specific sensor data, additional energy harvesting circuitry is required to drive the modulation module, which greatly increases the size of the device [16], [17], [18]. The diode-based harmonic transponders generate harmonics while also producing dc power that is often wasted. Therefore, the design of a compact harmonic transponder with dc power supply capability based on the diodes is proposed here. The single-port design described in Section III is used in the design so that the transponder can operate with only one antenna, further reducing the size.

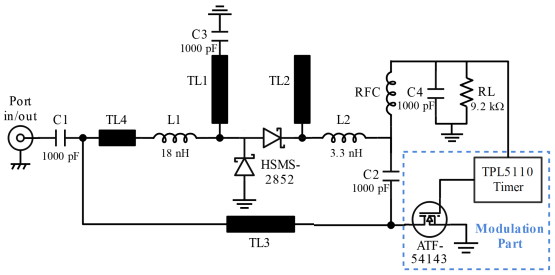

Fig. 11. Schematic of the proposed single-port harmonic transponder with modulation capability.

A schematic of the proposed harmonic transponder with dc power supply capability is shown in Fig. 11. Since this battery-free system is designed to be used at low power levels (<0 dBm), a voltage doubler is used to boost the rectified voltage to drive other modules. The voltage doubler can provide twice the voltage of a single diode structure at the same input power without additional boost circuits or power management modules. The diodes used are HSMS-2850 ones which have good performance at the power level of interest, while an HSMS-2852 is a chip with two diodes.

To make use of the harmonic generation and RF-dc rectification capabilities of the diode, some modification to the circuit is needed. Since the short stub TL_1 will affect the energy storage function of the capacitor C_4, the end of the stub TL_1 is first connected to a dc block capacitor C_3 and then connected to the ground, so that the dc path can be blocked without affecting the RF path. Due to changes in the diode used and the expected input power, the value of the inductor used for matching also needs to be adjusted accordingly. In the dc output port, an RF choke RFC is used as a lowpass filter. The RF choke also prevents the output capacitor C_4 from bypassing the second harmonic to the ground. The output capacitor C_4 connected in parallel with the load resistor R_L plays the role of controlling the ripple and smoothing the dc output voltage.

The proposed compact single-port harmonic transponder with dc power supply capability is designed to operate at 2.4 GHz and fabricated on a 1.524-mm thick RO4003C substrate ($\varepsilon_r = 3.55$) as shown in Fig. 12. The RF to dc conversion efficiency is defined as

$$\eta = \left(\frac{V_{\mathrm{out}}^2}{R_L P_{\mathrm{in}}}\right) \times 100\% \tag{4}$$

where V_{out} is the dc voltage across the load resistor R_L and P_{in} is the input RF power. The results of the harmonic balance simulation using ADS are shown in Fig. 13. From the results, under the load condition of 8 to 10 kΩ, the performance is relatively stable. The proposed design with a load of 9.2 kΩ can achieve 60% peak RF-dc conversion efficiency at 3 dBm input power and can provide up to 3.4 V dc output voltage. The detailed parameters of the components used are shown in Fig. 11. The simulated and measured power conversion loss of the second harmonic generation as a function of input power is shown in Fig. 14. The proposed design can achieve a conversion loss of no more than 15 dB when the input power

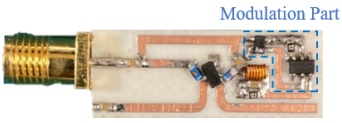

Fig. 12. Photograph of the proposed single-port harmonic transponder with modulation capability.

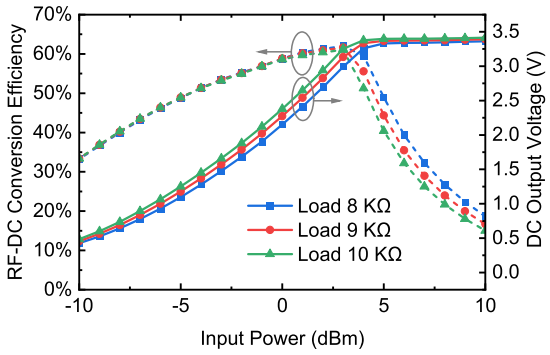

Fig. 13. Simulated RF-dc conversion efficiency and output dc voltage of the proposed single-port harmonic transponder with dc power supply capability.

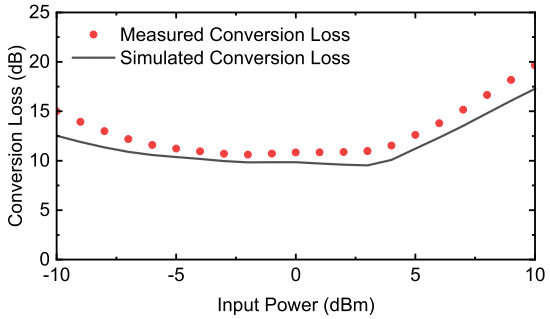

Fig. 14. Simulated and measured second harmonic power conversion loss of the proposed single-port harmonic transponder with dc power supply capability.

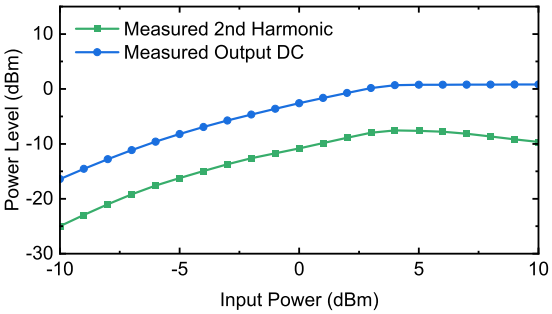

Fig. 15. Measured dc output power and the second harmonic power of the proposed single-port harmonic transponder with dc power supply capability.

is between –10 and 7 dBm. The parasitic behavior of surface mount components and manufacturing errors that are not fully accounted for in the simulation can cause subtle differences between the simulated and measured conversion losses. Fig. 15 shows the measured dc output power and the second harmonic power at different input power levels. The proposed design can generate a peak harmonic level of −7.5 dBm at an input power of 4 dBm. Fig. 16 shows the measured dc voltage in relation to the dc output power. The proposed circuit can provide a voltage of up to 3.5 V and a power of about 1.5 mW.

Table II compares the performance of the proposed harmonic transponder with dc power supply capability with previous works. Compared with other dual-port designs capable of generating both harmonics and dc power, the measured

TABLE II
COMPARISON OF THE PROPOSED COMPACT SINGLE-PORT HARMONIC TRANSPONDER WITH DC POWER SUPPLY CAPABILITY AND RELATED DESIGNS

Reference	2017 [19]	2018 [20]	2021 [21]	**This work**
Frequency GHz	0.915	2.6	0.915	**2.4**
Diode	HSMS-2865	HSMS-2862	HSMS-2860	**HSMS -2852**
Port	Dual port	Dual port	Dual port	**Single port**
Harmonic power level @ 0 dBm	-46 dBm	-19 dBm	-14 dBm	**-12 dBm**
RF to DC conversion efficiency @ 0 dBm	25%	50%	35%	**54%**
Overall energy conversion rate @ 0 dBm	25%	51%	39%	**60%**

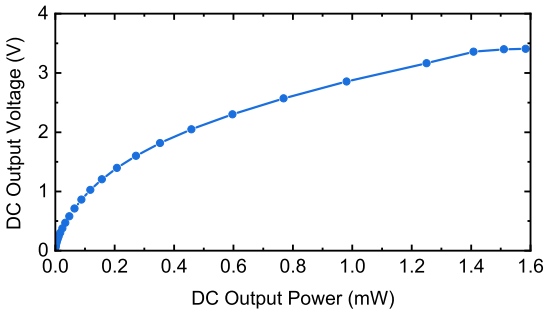

Fig. 16. Measured dc voltage in relation to the dc output power of the proposed single-port harmonic transponder with dc power supply capability.

harmonic power and RF to dc conversion efficiency of the proposed single-port design can remain relatively high at an input power level of 0 dBm. The overall energy conversion rate (OECR), by taking account of both RF to dc and f_0 to $2f_0$ conversion, can be calculated as follows:

$$\mathrm{OECR} = \left(\frac{P_{2f_0} + V_{\mathrm{out}}^2 / R_L}{P_{f_0}} \right) \times 100\% \tag{5}$$

where P_{f_0} is the input power at the fundamental frequency and P_{2f_0} is the output power at the second harmonic. At the input power level of 0 dBm, the proposed compact single-port transponder with dc power supply capability can provide a high OECR as well.

In order to better demonstrate the potential of the proposed transponder architecture for low-power IoT applications, a harmonic transponder with On-Off Keying (OOK) modulation has been designed, as shown in the blue dashed box in Fig. 11. A nano-power timer TPL5110 was used to generate square wave signals for modulation. The timer was powered by the dc output of the harmonic transponder with dc power supply capability. The required supply voltage of a TPL5110 timer is from 1.8 to 5.5 V, and the typical power needed is about 90 nW. A transistor ATF-54143 is connected in parallel acting as a switch. The square wave signal from the timer is used to drive the gate of the transistor. When the signal is logic low, the transistor is an open circuit, the harmonic can pass through. When the signal is logic high, the transistor is turned on, and the harmonic will be short-circuited to the ground.

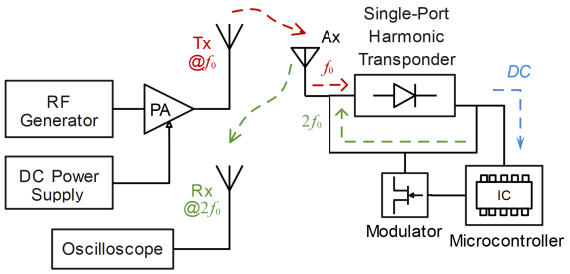

Fig. 17. Block diagram of the experimental setup for proposed single-port harmonic transponder with modulation capability.

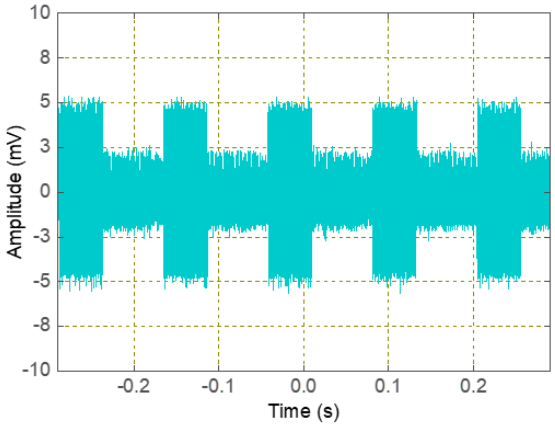

Fig. 18. Received modulated harmonic waveform from the proposed harmonic transponder with the OOK modulation capability.

Since the switch is separated from the input and output ports by a quarter-wavelength transmission line, even when it is in a short-circuited state, it will be converted to an open circuit at the fundamental frequency. Thus, the additional switch will not affect the fundamental frequency input from the port.

Fig. 12 shows the fabricated harmonic transponder with the OOK modulation capability. It was designed to operate at 2.4 GHz and fabricated on a RO4003C substrate. Fig. 17 shows the block diagram of the experimental setup for the proposed harmonic transponder modulated by a timer-driven switch. The signal analyzer was replaced by an oscilloscope to display the modulated waveform. A bandpass filter with a center frequency of $2f_0$ was placed between the antenna and the oscilloscope to filter out the fundamental frequency signal. The harmonic transponder was placed 1.8 m away from the receiving antenna. By adjusting the power level of the transmitter at the base station, the effective isotropic radiated power from the Tx antenna was 36 dBm. At this time, the received RF power by the harmonic transponder was 0 dBm, and the dc output power was 0.5 mW with a voltage of 2 V. It can meet the power supply requirements of the chip, that is, the power is greater than 0.09 mW and the voltage is higher than 1.8 V. The modulated harmonic signal received by the oscilloscope is shown in Fig. 18. The harmonic signal has been modulated by the ON-OFF clock signal from a timer TPL5110. Due to the modulation scheme in which the output port is connected in parallel, the transistor is not completely grounded when it is turned on, and its ON-resistance will cause part of the signal to leak to the output port. This makes the modulation depth less than 100%, but its high and low levels can be clearly distinguished. The TPL5110 can only provide a minimum time interval of 100 ms, thus the clock rate is 10 Hz. This timer can be replaced with any encoder or sensor with similar or lower power consumption without modifications to the front circuit. It can be seen that the dc power provided by the proposed harmonic transponder with dc power supply capability can provide dc power to an add-on chip and provide a harmonic signal as a carrier for communications.

V. Conclusion

This article has reported a new architecture for the design of compact single-port harmonic transponders. The proposed diplexing structure based on stubs and transmission lines eliminates the need for a diplexer in single-port harmonic transponders. The network can provide excellent isolation between the fundamental frequency and second harmonic signals. Compared to a single-resonator-based diplexer, the proposed network has a lower insertion loss, a wider bandwidth, and a more compact size. Due to the simplicity of the structure, the transmission line can be folded to reduce the area further without compromising performance too much.

This diplexing structure can also be used to design a compact single-port harmonic transponder with dc power supply capability, achieving the goal of operating with a single antenna while maintaining a compact structure. A simple OOK communication system based on the proposed design has been constructed to demonstrate the usefulness of the proposed method. In the actual test, the dc power obtained by the harmonic transponder successfully modulated the second harmonic. It has been proven that the harmonic transponder with the proposed architecture is a very promising solution for future low-power IoT applications.

References

[1] M. Saikat, K. Deepak, and C. Premjeet, "Recent advances and applications of passive harmonic RFID systems: A review," *Micromachines*, vol. 12, p. 420, Apr. 2021.

[2] J. Shefer and R. J. Klensch, "Harmonic radar helps autos avoid collisions," *IEEE Spectr.*, vol. S-10, no. 5, pp. 38–45, May 1973.

[3] J. R. Riley and A. D. Smith, "Design considerations for an harmonic radar to investigate the flight of insects at low altitude," *Comput. Electron. Agricult.*, vol. 35, nos. 2–3, pp. 151–169, Aug. 2002.

[4] M. Bouthinon, J. Gavan, and F. Zadworny, "Passive microwave transposer, frequency doubler for detecting the avalanche victims," in *Proc. 10th Eur. Microw. Conf.*, Warszawa, Poland, Sep. 1980, pp. 579–583.

[5] N. Barbot and S. Tedjini, "Towards identification for harmonic transponders," in *Proc. 3rd URSI Atlantic Asia Pacific Radio Sci. Meeting (AT-AP-RASC)*, May 2022, pp. 1–3.

[6] V. Palazzi et al., "Low-power frequency doubler in cellulose-based materials for harmonic RFID applications," *IEEE Microw. Wireless Compon. Lett.*, vol. 24, no. 12, pp. 896–898, Dec. 2014.

[7] V. Palazzi, F. Alimenti, C. Kalialakis, P. Mezzanotte, A. Georgiadis, and L. Roselli, "Highly integrable paper-based harmonic transponder for low-power and long-range IoT applications," *IEEE Antennas Wireless Propag. Lett.*, vol. 16, pp. 3196–3199, 2017.

[8] X. Gu, N. N. Srinaga, L. Guo, S. Hemour, and K. Wu, "Diplexer-based fully passive harmonic transponder for sub-6-GHz 5G-compatible IoT applications," *IEEE Trans. Microw. Theory Techn.*, vol. 67, no. 5, pp. 1675–1687, May 2019.

[9] X. Gu, W. Lin, S. Hemour, and K. Wu, "Readout distance enhancement of battery-free harmonic transponder," *IEEE Trans. Microw. Theory Techn.*, vol. 69, no. 7, pp. 3413–3424, Jul. 2021.

[10] J. Zhang, S. D. Joseph, Y. Huang, and J. Zhou, "Design of a compact harmonic transponder based on quarter-wavelength impedance transformers," in *Proc. 51st Eur. Microw. Conf. (EuMC)*, Apr. 2022, pp. 680–683.

[11] S. D. Joseph, "Rectennas for wireless energy harvesting and power transfer," Ph.D. dissertation, Dept. Electr. Electron. Eng., Univ. Liverpool, Liverpool, U.K., Jun. 2021.

[12] Y.-H. Suh and K. Chang, "A high-efficiency dual-frequency rectenna for 2.45- and 5.8-GHz wireless power transmission," *IEEE Trans. Microw. Theory Techn.*, vol. 50, no. 7, pp. 1784–1789, Jul. 2002.

[13] MVG, Marietta, GA, USA. (2018). *Dual-Ridge Horns*. Accessed: Dec. 5, 2022. [Online]. Available: https://www.mvg-world.com/upload/media/products_document/0001/01/2da49fe7fa1305cb3484d6795a857fe3e6cd5c7a.pdf

[14] V. Palazzi et al., "Demonstration of a chipless harmonic tag working as crack sensor for electronic sealing applications," *Wireless Power Transf.*, vol. 2, pp. 1–8, Oct. 2015.

[15] B. Kubina, J. Romeu, C. Mandel, M. Schußler, and R. Jakoby, "Design of a quasi-chipless harmonic radar sensor for ambient temperature sensing," in *Proc. IEEE Sens. Conf.*, Nov. 2014, pp. 1567–1570.

[16] S. Mondal and P. Chahal, "A passive harmonic RFID tag and interrogator development," *IEEE J. Radio Freq. Identificat.*, vol. 3, no. 2, pp. 98–107, Jun. 2019.

[17] A. Lazaro, R. Villarino, and D. Girbau, "A passive harmonic tag for humidity sensing," *Int. J. Antennas Propag.*, vol. 2014, pp. 1–11, Jul. 2014.

[18] A. Abdelnour, A. Lazaro, R. Villarino, D. Kaddour, S. Tedjini, and D. Girbau, "Passive harmonic RFID system for buried assets localization," *Sensors*, vol. 18, no. 11, p. 3635, Oct. 2018.

[19] C.-J. Peng, S.-F. Yang, A.-C. Huang, T.-H. Huang, P.-J. Chung, and F.-M. Wu, "Harmonic enhanced location detection technique for energy harvesting receiver with resonator coupling design," in *Proc. IEEE Wireless Power Transf. Conf. (WPTC)*, May 2017, pp. 1–3.

[20] T. Ngo and T. Yang, "Harmonic-recycling rectifier design for localization and power tuning," in *Proc. IEEE Wireless Power Transf. Conf. (WPTC)*, Jun. 2018, pp. 1–4.

[21] S. D. Joseph, Y. Huang, S. S. H. Hsu, A. Alieldin, and C. Song, "Second harmonic exploitation for high-efficiency wireless power transfer using duplexing rectenna," *IEEE Trans. Microw. Theory Techn.*, vol. 69, no. 1, pp. 482–494, Jan. 2021.

Jinyao Zhang received the B.Eng. degree (Hons.) in electrical and electronic engineering from the University of Liverpool, Liverpool, U.K., in 2018, where he is currently pursuing the Ph.D. degree in RF and microwave engineering.

His research interests include rectifiers, harmonic transponders, microwave circuit designs, wireless power transfer, and energy harvesting.

Sumin David Joseph received the B.Tech. degree (Hons.) in electronics and communication from CUSAT University, Kochi, India, in 2012, the M.Tech. degree (Hons.) in communication systems from the Visvesvaraya National Institute of Technology, Nagpur, India, in 2015, and the Dual Ph.D. degree (Distinction) in electrical engineering from the University of Liverpool, Liverpool, U.K., and the National Tsing Hua University, Hsinchu, Taiwan, in 2021.

He is currently working as a Post-Doctoral Research Associate with The University of Sheffield, Sheffield, U.K. He was a Lab Engineer under CoE with the Visvesvaraya National Institute of Technology, from 2015 to 2017, where he was involved in projects of national importance. He has authored or coauthored more than 25 articles in peer-reviewed journals and conference proceedings. His research interests include self-biased circulators, mm-wave antenna arrays, rectifying antennas, MMIC circuits, RFIC, rectifiers, integrated circuit designs, flexible electronics, wireless power transfer, energy harvesting, and TMA antenna arrays.

Dr. Joseph is a Technical Reviewer for leading academic journals and conferences, including IEEE TRANSACTIONS OF ANTENNAS AND PROPAGATION, IEEE ANTENNAS AND WIRELESS PROPAGATION LETTERS, and IEEE ACCESS.

Yi Huang (Fellow, IEEE) received the B.Sc. degree in physics, Wuhan University, Wuhan, China, in 1984, the M.Sc.Eng. degree in microwave engineering, Nanjing, China, in 1987, and the D.Phil. degree in communications from the University of Oxford, Oxford, U.K., in 1994.

He has been conducting research in the areas of antennas, wireless communications, applied electromagnetics, radar, and EMC, since 1987. More recently, he is focused on new materials for antennas, wireless energy harvesting, and power transfer. His experience includes three years spent with NRIET, Nanjing, as a Radar Engineer and various periods with the Universities of Birmingham, Oxford, and Essex, U.K. as a member of research staff. He worked as a Research Fellow at British Telecom Labs, Ipswich, U.K., in 1994 and then joined the Department of Electrical Engineering and Electronics, University of Liverpool, Liverpool, U.K., as a Faculty, in 1995, where he is now a Full Professor in wireless engineering, the Head of High-Frequency Engineering Group. He has published over 500 refereed articles in leading international journals and conference proceedings and authored four books, including *Antennas: From Theory to Practice* (John Wiley, 2008, 2021). He has received many patents, and research grants from research councils, government agencies, charities, EU, and industry.

Prof. Hung was a recipient of over ten awards (e.g., BAE Systems Chairman's Award 2017, IET, and Best Paper Awards). He has served on a number of national and international technical committees and has been an Editor, Associate Editor, or Guest Editor of five international journals. In addition, he has been a keynote/invited speaker and organizer of many conferences and workshops (e.g., IEEE iWAT2010, LAPC2012, and EuCAP2018). He is at present the Editor-in-Chief of Wireless Engineering and Technology, an Associate Editor of IEEE ANTENNAS AND WIRELESS PROPAGATION LETTERS, U.K. and Ireland Rep to the European Association of Antenna and Propagation (EurAAP), form 2016 to 2020, a Fellow of IET and a Distinguished Lecturer of IEEE AP-S.

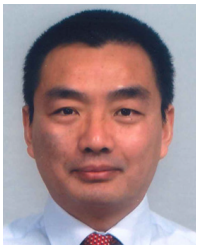

Jiafeng Zhou received the B.Sc. degree in radio physics from Nanjing University, Nanjing, China, in 1997, and the Ph.D. degree from the University of Birmingham, Birmingham, U.K., in 2004, where his research concerned high-temperature superconductor microwave filters.

Since July 1997, for two and a half years he has been with the National Meteorological Satellite Centre of China, Beijing, China, where he was involved with the Development of Communication Systems for Chinese Geostationary Meteorological Satellites. From August 2004 to April 2006, he was a Research Fellow with the University of Birmingham, where his research concerned phased arrays for reflector observing systems. Then he moved to the Department of Electronic and Electrical Engineering, University of Bristol, Bristol, U.K., until August 2013. His research in Bristol was on the development of highly efficient and linear amplifiers. He is currently with the Department of Electrical Engineering and Electronics, University of Liverpool, Liverpool, U.K. His research interests include microwave power amplifiers, filters, electromagnetic energy harvesting, and wireless power transfer.